

Dalton Transactions

Accepted Manuscript



This is an *Accepted Manuscript*, which has been through the Royal Society of Chemistry peer review process and has been accepted for publication.

Accepted Manuscripts are published online shortly after acceptance, before technical editing, formatting and proof reading. Using this free service, authors can make their results available to the community, in citable form, before we publish the edited article. We will replace this *Accepted Manuscript* with the edited and formatted *Advance Article* as soon as it is available.

You can find more information about *Accepted Manuscripts* in the [Information for Authors](#).

Please note that technical editing may introduce minor changes to the text and/or graphics, which may alter content. The journal's standard [Terms & Conditions](#) and the [Ethical guidelines](#) still apply. In no event shall the Royal Society of Chemistry be held responsible for any errors or omissions in this *Accepted Manuscript* or any consequences arising from the use of any information it contains.

Silver Coordination Polymers with Tri- and Hexacyanoethyl-functionalized Macrocyclic Ligands

Zhen Ma ^{a,b,*}, Huaduan Shi ^a, Xiuqiang Deng ^a, M. Fátima C. Guedes da Silva ^{b,c,*}, Luísa M. D. R. S. Martins, ^{b,c} and Armando J. L. Pombeiro ^b

^a Guangxi Key Laboratory of Petrochemical Resource Processing and Process Intensification Technology, School of Chemistry and Chemical Engineering, Guangxi University, Nanning 530004, P. R. China, E-mail: mzmz2009@sohu.com

^b Centro de Química Estrutural, Complexo I, Instituto Superior Técnico, Universidade de Lisboa, Av. Rovisco Pais, 1049-001, Lisbon, Portugal, E-mail: fatima.guedes@tecnico.ulisboa.pt

^c Chemical Engineering Department, ISEL, R. Conselheiro Emídio Navarro, 1959-007 Lisboa, Portugal.

Abstract

Tri- and hexa-cyanoethyl functionalized 17- (**L**¹) and 42-membered (**L**²) macrocyclic compounds were obtained by [1+1] (for **L**¹) or [2+2] (for **L**²) cyclocondensation of the corresponding dialdehyde and diethylenetriamine, followed by hydrogenation by KBH₄ and subsequent cyano-functionalization with acrylonitrile. They react with silver nitrate leading to the formation of [AgL¹](NO₃) (**1**) and of the metal-organic coordination polymers [Ag₂(NO₃)₂L¹]_n (**2**) and {[Ag₂L²](NO₃)₂]_n (**3**), respectively. The complexes were characterized by elemental analysis, ¹H NMR, ¹³C NMR, IR spectroscopies, and ESI-MS, and, for **L**², **1**, **2** and **3**, also by single crystal X-ray diffraction. The metal cation in **1** is pentacoordinated with a N₃O₂ coordination environment, while in **2** the metal cations display N₄O₂ octahedral and N₂O₃ square-pyramid coordination, and in **3** they are in square-planar N₄ sites. In **1**, the ligand acts as a pentadentate chelator and, in the other two cases, the ligands behave as octadentate chelators in a 1κ³N:κ²O,2κN,3κN,4κN (in **2**) or 1κ³N,2κ³N,3κN,4κN fashion (in **3**). The cyanoethyl strands of the ligands are directly involved in the formation of the 2D frameworks of **2** and **3**, which in the former polymer can be viewed as a net composed of hexametallc 36-membered macrocyclic rings, and in the latter generates extra hexametallc 58-membered cyclic sets that form zig-zag layers.

The thermal analytical and electrochemical properties of these silver complexes were also studied.

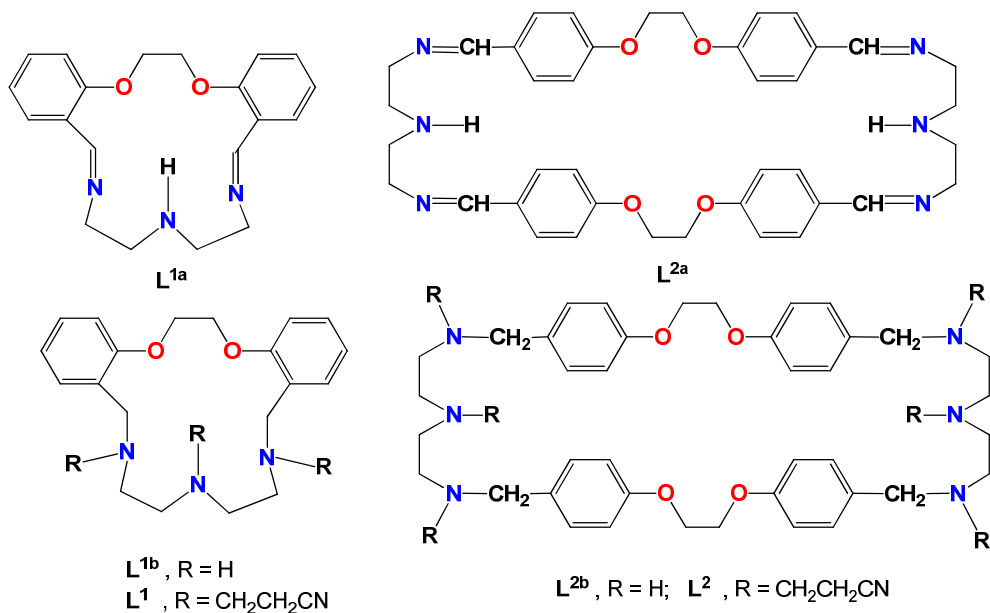
Introduction

Functionalization of polyaza macrocyclic and macrobicyclic compounds by several chemical groups, such as acrylonitrile, [1-6] alkynyl, [7] phosphanylmethyl, [8] carboxyl, [9] and heterocycles [10], on their secondary N-sites, has attracted a considerable interest, and a number of their complexes has been prepared with different metal ions, with interesting properties in the fields of coordination chemistry, electrochemistry, photoluminescence and catalysis [11-17]. We have also engaged in this investigation [9, 15] searching for new synthetic procedures that may allow designing a diversity of transition metal complexes with such a type of ligands, aiming to prepare novel structures with relevance in material and medicinal chemistries.

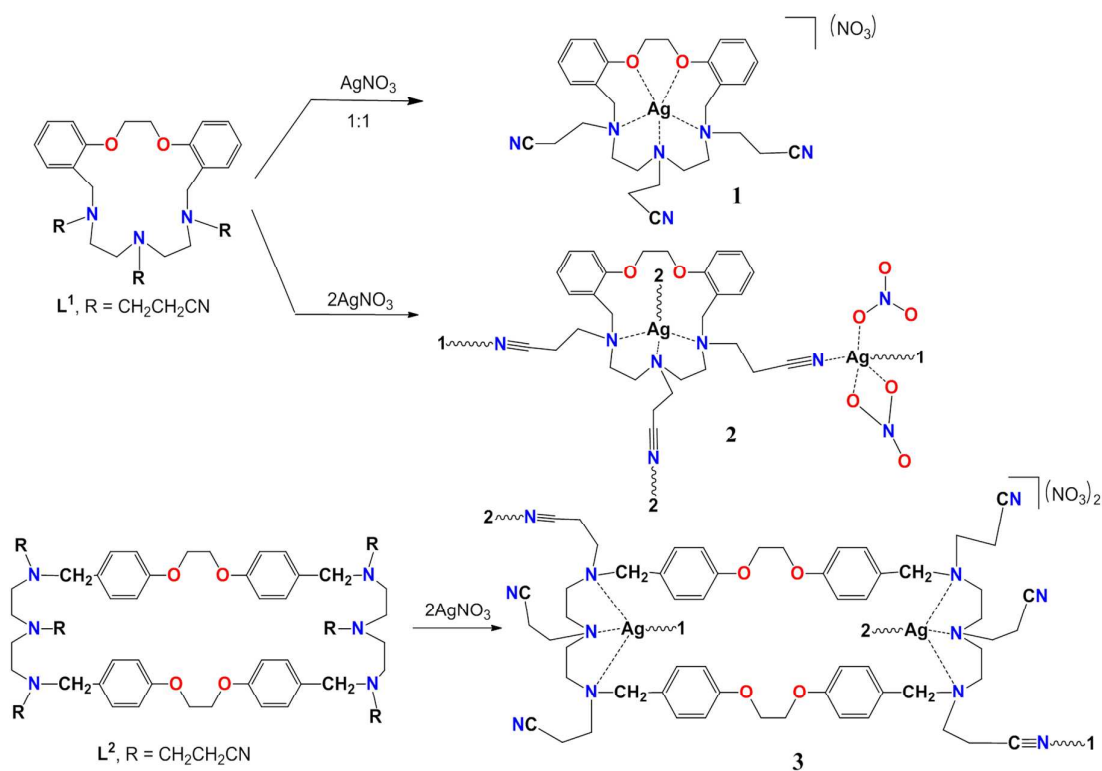
It is well known that silver complexes are good candidates for antibacterial or antitumor activities, and can show interesting electrochemical and catalytic properties [18]. Unfortunately, one shortcoming of the compounds with this metal is their usual instability in air, limiting their applications. In this work, we aim to synthesize stable silver(I) complexes with ligands that combine advantages of macrocyclic and nitrile compounds, which are expected to show effective coordination abilities to this metal ion, and study their thermal and electrochemical properties.

We report herein two new tri- and hexa-cyanoethyl functionalized macrocycles, L^1 and L^2 , which were synthesized by the reaction of the two polyaza macrocyclic precursors L^{1b} and L^{2b} (Scheme 1) with acrylonitrile according to a previously reported general procedure [1,19a]. Depending on the ligand and on the $AgNO_3$: ligand molar ratios, the reaction of L^1 or L^2 with $AgNO_3$ afforded the mononuclear complex $[AgL^1](NO_3)$ (**1**) or the polymeric compounds $[Ag_2(NO_3)_2L^1]_n$ (**2**) or $\{[Ag_2L^2](NO_3)_2\}_n$ (**3**), which represent rare examples of stable silver cyanoethyl functionalized coronand polymeric complexes. In **2**, L^1 is coordinated to four silver

ions, resulting in hexanuclear metallic macrocyclic motifs and a 2-D structure. In **3**, L^2 binds two silver ions in its cavity and is coordinated to two other neighbouring ones, forming interesting cylindrical motifs and a 2-D layer.



Scheme 1 Ligands L^1 and L^2 , and their precursors



Scheme 2 Synthetic routes to **1**, **2** and **3**

Experimental

Instrumentation and reagents

All reagents were of analytical grade or purified by standard methods. C, H and N elemental analyses were carried out on a Vario EL III Elemental Analyzer. Infrared spectra (4000–400 cm^{-1}) were recorded on a BIO-RAD FTS 3000MX or a Bruker IFS 1113v in KBr pellets (abbreviations: vs – very strong, s – strong, m – medium, w – weak, br – broad, sh – shoulder). ^1H and ^{13}C NMR spectra were run on a Varian Unity 400 spectrometer at ambient temperature. TG-DTA data were collected with a Perkin Elmer STA6000 Thermal Analyzer at a heating rate of 10 K min^{-1} under an air atmosphere. Electrospray mass spectra (ESI-MS) were run (in NCMe for L^1 and L^2 , or in a mixture of MeOH/DMSO for complexes **1-3**) with an ion-trap instrument (Varian 500-MS LC Ion Trap Mass Spectrometer) equipped with an electrospray ion source. For electrospray ionization, the drying gas and flow rate were optimized according to the particular sample with 35 psi nebulizer pressure. Scanning was performed from m/z 100 to 1200 for L^1 , L^2 , **1** and **2** and m/z 100 to 1500 for **3**.

The electrochemical experiments were performed on an EG&G PAR 273A potentiostat/galvanostat connected to a personal computer through a GPIB interface. Cyclic voltammetry (CV) studies were undertaken in 0.2 M [$^n\text{Bu}_4\text{N}$][BF_4]/NCMe, at a platinum disc working electrode ($d = 0.5$ mm) and at room temperature. Controlled-potential electrolyses (CPE) were carried out in electrolyte solutions with the above-mentioned composition, in a three-electrode H-type cell. The compartments were separated by a sintered glass frit and equipped with platinum gauze working and counter electrodes. For both CV and CPE experiments, a Luggin capillary connected to a silver wire pseudo-reference electrode was used to control the working electrode potential. A Pt wire was employed as the counter-electrode for the CV cell. The CPE experiments were monitored regularly by CV, thus assuring no significant potential drift occurred along the electrolysis. The solutions were saturated with N_2 by bubbling this gas before each run, the redox potentials of the complexes were measured by CV

in the presence of ferrocene as the internal standard, and their values are quoted relative to the SCE by using the $[\text{Fe}(\eta^5\text{-C}_5\text{H}_5)_2]^{0/+}$ redox couple ($E_{1/2}^{\text{ox}} = 0.42 \text{ V vs. SCE}$) [20].

General Synthetic Procedure

Scheme 1 represents the two ligands L^1 and L^2 , whose isolation and full characterization were achieved in this work for the first time. Their synthetic precursors (L^{1a} , L^{1b} , L^{2a} and L^{2b}) were synthesized by following the methods earlier reported [19], via [1+1] or [2+2] condensation of diethylenetriamine with 2,2'-(ethane-1,2-diylbis(oxy))dibenzaldehyde or 4,4'-(ethane-1,2-diylbis(oxy))-dibenzaldehyde, respectively, followed by hydrogenation with KBH_4 .

Synthesis of L^1

3.4 g (0.010 mol) of L^{1b} were heated to 55 °C in 200 mL of methanol until total dissolution. Upon addition of 0.48 g (9.0 mmol) of acrylonitrile the mixture was refluxed for 24 h. After most of the solvent (ca. 150 mL) was distilled off and the system stored overnight at room temperature, colourless crystals of L^1 were obtained (4.5 g, yield 90 %). m.p. 98 - 99 °C. Anal. calcd for $\text{C}_{29}\text{H}_{36}\text{N}_6\text{O}_2$ (500.64): C, 69.57; H, 7.25; N, 16.79. Found C, 69.74; H, 7.51; N, 16.57. ESI-MS: $[\text{L} + \text{H}^+]^+$: (501.3, 25 %), $[\text{L} - \text{C}_3\text{H}_4\text{N} + \text{H}^+]^+$: (448.4, 100 %). ^1H NMR (400 MHz, CDCl_3), δ 2.17 (t, $J = 6.8 \text{ Hz}$, 2H, $-\text{CH}_2\text{CN}$), 2.43-2.51 (m, 10H, $-\text{CH}_2\text{CH}_2\text{CN}$), 2.59 (t, $J = 6.4 \text{ Hz}$, 4H, $-\text{NCH}_2\text{CH}_2\text{N}$), 2.82 (t, $J = 7.0 \text{ Hz}$, 4H, $-\text{NCH}_2\text{CH}_2\text{N}$), 3.69 (s, 4H, $-\text{CH}_2\text{Ar}$), 4.37 (s, 4H, $-\text{OCH}_2$), 6.91-6.98 (m, 4H, aryl), 7.27-7.32 (m, 4H, aryl). ^{13}C NMR (100 MHz, CDCl_3), δ 16.77 ($\text{CH}_2\text{CH}_2\text{-CN}$), 50.22 ($\text{CH}_2\text{CH}_2\text{N}$), 50.59 ($\text{CH}_2\text{CH}_2\text{N}$), 52.29 ($\text{CH}_2\text{CH}_2\text{-CN}$), 53.11 ($-\text{CH}_2\text{-aryl}$), 67.00 (O-CH_2); 111.41 (aryl), 119.40 ($-\text{CN}$), 120.90 (aryl), 127.27 ($-\text{CH}_2\text{-aryl}$), 128.74 (aryl), 131.10 (aryl), 157.10 ($-\text{O-aryl}$). IR (KBr disc) (cm^{-1}): 3065 (w), 2947 (s), 2908 (s), 2809 (s), 2846 (m), 2810 (vs), 2239 (s), 1599 (s, $\nu_{\text{aryl-H}}$), 1587 (m), 1493 (s, $\nu_{\text{aryl-H}}$), 1452 (s), 1377 (m), 1340 (m), 1291 (m), 1244 (vs), 1196 (m), 1113 (s), 1100 (s), 1069 (m), 1048 (m), 1009 (m), 954 (s), 925 (m), 951 (s), 758 (s), 721 (w), 620 (w).

Synthesis of L^2 0.20 g (0.29 mmol) of L^{2b} and 40 mL of ethanol were mixed in a 100 mL flask and a white emulsion was obtained. Upon addition of 0.48 g (9.0 mmol) of acrylonitrile the mixture was refluxed for 24 h and the initially colourless solution turned to pale yellow. The hot solution was filtered and, upon cooling, colourless crystals of L^2 were formed which were separated by filtration and dried (0.20 g, 69 %). m.p. 123-125 °C. Anal. calcd for $C_{58}H_{72}N_{12}O_4 \cdot C_2H_5OH$ (1047.34): C, 68.81 H, 7.50; N, 16.05. Found C, 68.55; H, 7.65; N, 16.12. ESI-MS: $[L + H^+]^+$: (1001.4, 10 %), $[L - C_3H_4N + H^+]^+$: (948.8, 100 %). 1H NMR (400 MHz, $CDCl_3$), δ 2.35-2.42 (m, $J = 7.0$ Hz, 12H, $-NCH_2$), 2.49-2.51 (m, $J = 3.2$ Hz, 16H, $-NCH_2CH_2N$), 2.72-2.77 (q, $J = 6.5$ Hz, 12H, $-CH_2CN$), 3.47 (s, 8H, $-CH_2Ar$), 4.15 (s, 8H, $-OCH_2$), 6.85 (d, $J = 8.4$ Hz, 8H, aryl), 7.20 (d, $J = 8.8$ Hz, 8H, aryl). ^{13}C NMR (100 MHz, $CDCl_3$), δ 16.95 (CH_2CH_2-CN), 17.18 (CH_2CH_2-CN), 50.15 (CH_2CH_2-CN), 50.80 (CH_2CH_2-CN), 52.05 ($-NCH_2CH_2N$), 52.74 ($-NCH_2CH_2N$), 58.45 ($-CH_2-aryl$), 66.73 ($O-CH_2$), 114.75 (aryl), 119.34 ($-CN$), 130.25 (aryl), 131.16 (CH_2-aryl), 158.19 ($-O-aryl$). IR (KBr disc) (cm^{-1}): 3043 (w), 2942 (s), 2925 (s), 2923 (s), 2249 (s), 1609 (s, ν_{aryl-H}), 1510 (vs, ν_{aryl-H}), 1456 (s), 1421 (w, ν_{aryl-H}), 1372 (m), 1302 (w), 1244 (s), 1229 (s), 1173 (m), 1119 (s), 1075 (s), 1018 (m), 947 (s), 822 (s), 770 (m), 628 (w), 518 (m).

Suitable crystals for X-ray diffraction analysis were obtained by slow evaporation of an acetonitrile solution of L^2 .

Synthesis of $[AgL^1](NO_3)$ (1)

A solution of $AgNO_3$ (0.085, 0.50 mmol) in 10 mL acetonitrile in a 50 mL flask was heated to 55 °C to dissolve the silver salt. A 10 mL dichloromethane solution of L^1 (0.25g, 0.50 mmol) was added dropwise. The system was stirred for 24 h at this temperature. After cooling to room temperature and filtration, diffusion of diethyl ether into the filtrate led to colourless crystals of **1** suitable for X-ray determination (0.17 g, 51 % yield based on the silver salt). Anal. calcd for $C_{29}H_{36}Ag_1N_7O_5$ (670.51): C, 51.95; H, 5.41; N, 14.62. Found: C, 51.94; H, 5.50; N, 14.66. TG-DTA, Ag_2O % 18.4; Calc for Ag_2O % is 17.3. ESI-MS (DMSO): $[AgL^1]^+$: (609.2, 100 %). 1H NMR (400 MHz, $CDCl_3$), δ 2.29 (s, 2H, $-NCH_2$), 2.55-2.93 (m, 18H, CH_2N- and $-CH_2CN$),

3.78 (s, 4H, CH_2Ar), 4.52 (s, 4H, $O-CH_2$), 7.04 (t, $J = 7.2$ Hz, 2H, aryl), 7.19 (d, $J = 8.0$ Hz, 2H, aryl), 7.35 (d, $J = 7.2$ Hz, 2H, aryl), 7.41 (t, $J = 6.4$ Hz, 2H, aryl). IR (KBr disc) (cm^{-1}): 2930 (s), 2851 (s), 2247 (m), 1601 (m, ν_{aryl-H}), 1494 (s, ν_{aryl-H}), 1451 (s), 1383 (vs), 1344 (vs), 1238 (s), 1196 (m), 1122 (m), 1053 (m), 943 (s), 766 (s), 624 (w).

Synthesis of $[Ag_2(NO_3)_2L^1]_n$ (2)

A solution of $AgNO_3$ (0.17 g, 1.00 mmol) in 10 mL acetonitrile in a 50 mL flask was heated to 55 °C to dissolve the silver salt. A 10 mL dichloromethane solution of L^1 (0.25g, 0.50 mmol) was added dropwise. The system was stirred for 24 h at this temperature. After cooling to room temperature and filtration, diffusion of diethyl ether into the filtrate led to colourless crystals of **2** suitable for X-ray determination (0.24 g, 57 % yield based on the silver salt). Anal. calcd for $C_{29}H_{36}Ag_2N_8O_8$ (840.38): C, 41.45; H, 4.32; N, 13.33. Found: C, 41.77; H, 4.36; N, 13.26. TG-DTA, Ag_2O % 27.3; Calc for Ag_2O % is 27.6. ESI-MS (DMSO): $[AgL^1]^+$: (607.6, 100 %), $[Ag(DMSO)_2C_2H_5CN]^+$: (319, 13 %), $[Ag(DMSO)C_2H_5CN]^+$: (243, 13 %). 1H NMR (400 MHz, $CDCl_3$), δ 2.08 (s, 6H, $-NCH_2$), 2.28 (s, 2H, $-CH_2N$), 2.39-2.72 (m, 12H, CH_2N - and $-CH_2CN$), 3.79 (s, 4H, CH_2Ar), 4.53 (s, 4H, $O-CH_2$), 7.04 (t, $J = 7.2$ Hz, 2H, aryl), 7.20 (d, $J = 8.4$ Hz, 2H, aryl), 7.35 (d, $J = 6.0$ Hz, 2H, aryl), 7.42 (t, $J = 7.6$ Hz, 2H, aryl). IR (KBr disc) (cm^{-1}): 3179 (w), 3114 (w), 3077 (m), 2957 (s), 2927 (s), 2863 (s), 2247 (s), 1601 (vs, ν_{aryl-H}), 1587 (s), 1496 (s, ν_{aryl-H}), 1449 (m), 1384 (m), 1292 (m), 1237 (m), 1124 (s), 1084 (m), 1069 (m), 1054 (m), 1030 (m), 935 (s), 819 (m), 778 (s), 760 (s), 723 (m), 632 (m), 552 (m), 479 (w).

Synthesis of $\{[Ag_2L^2](NO_3)_2\}_n$ (3)

A solution of $AgNO_3$ (0.085 g, 0.50 mmol) in 20 mL acetonitrile was added to 20 mL of a dichloromethane solution of L^2 (0.25 g, 0.25 mmol). The system was stirred for 24 h and a colourless solution formed. After filtration, diffusion of diethyl ether into the filtrate led to colourless crystals of **3** suitable for X-ray structural determination (0.12 g, 36 % yield based on silver nitrate).

Anal. calcd for $C_{58}H_{72}Ag_2N_{14}O_{10}$ (1341.02): C, 51.95; H, 5.41; N, 14.62. Found:

C, 51.45; H, 5.33; N, 14.50. TG-DTA, Ag₂O 17.3 %, calc Ag₂O % 17.3 %. ESI-MS (DMSO): [Ag₂L²(NO₃)]⁺: (1278.2, 6 %), [Ag₂L² – 2CH₂CH₂CN + H⁺]⁺ (1109.8, 100 %), [Ag(DMSO)₂]⁺: (264.6, 11 %). ¹H NMR (400 MHz, CDCl₃), δ 2.54 (s, 20H, -NCH₂), 2.74 (t, *J* = 4.8, 20H, -CH₂N- and -CH₂CN), 3.46 (s, 8H, CH₂Ar), 4.16 (s, 8H, O-CH₂), 6.89 (d, *J* = 8.4 Hz, 8H, aryl), 7.26 (d, *J* = 8.0 Hz, 8H, aryl). IR (KBr disc) (cm⁻¹): 2931 (m), 2852 (m), 2830 (m), 2427 (w), 2246 (m), 1611 (vs, ν_{aryl-H}), 1511 (vs, ν_{aryl-H}), 1455 (m), 1384 (vs), 1295 (m), 1235 (vs), 1172 (m), 1108 (m), 1072 (m), 941 (s), 830 (s), 776 (m), 522 (w).

X-ray Crystal Structure Determinations. Single crystals of L², **1**, **2** and **3** were mounted on glass fibers. Intensity data were collected using a Bruker AXS-KAPPA APEX II diffractometer with graphite monochromated Mo-Kα (λ 0.71073) radiation. Data were collected using omega scans of 0.5° per frame and full sphere of data were obtained. Cell parameters were retrieved using Bruker SMART software and refined using Bruker SAINT [21] on all the observed reflections. Absorption corrections were applied using SADABS [21]. Structures were solved by direct methods by using the SHELXS-97 package [22] and refined with SHELXL-97 [23]. Calculations were performed using the WinGX System-Version 1.80.03 [24]. The atomic positions of some methylene groups of **1**, and well of the O4 and O5 atom of the nitrate counter-ion, were disordered over two orientations and were refined with the use of PART instruction. The occupancies of the two components of each atom were refined to a ratio of 69% and 31%. In spite of this, the C57 and C58 carbon atom had to be refined isotropically. In compound **2** the positions of the methylene carbons C27 and C28 were also disordered over two orientations and refined with the use of PART instructions as well, their occupancies being refined to a ratio of 73% / 27% and 60% / 40 %, respectively. The positions of the hydrogen atoms bonded to the disordered carbon atoms were included in calculated positions by using the PART instructions in SHELXL and treated as riding atoms. The remaining hydrogen atoms were inserted in calculated positions. Least square refinements with anisotropic thermal motion parameters for all the non-hydrogen atoms and isotropic for the remaining atoms were employed.

CCDC 780498, 780499, 842196 and 936855 contain the supplementary crystallographic data of this paper. These data can be obtained free of charge from the Cambridge Crystallographic Data Centre via w.ccdc.cam.ac.uk/data_request/cif. Crystal data and details of data collections are reported in Table 1.

Results and discussion

The macrocyclic compounds L^{1b} and L^{2b} (Scheme 1) were prepared in high yields by [1+1] or [2+2] condensation of diethylenetriamine with 2,2'-(ethane-1,2-diylbis(oxy))dibenzaldehyde or 4,4'-(ethane-1,2-diylbis(oxy))-dibenzaldehyde, respectively, followed by hydrogenation with KBH_4 , in accord with a known method [1,2,19].

The cyanoethyl-functionalized ligands L^1 and L^2 were then obtained by reaction of L^{1b} or L^{2b} with acrylonitrile under reflux for 24 h in methanol or ethanol, respectively. They were isolated as air-stable white solids in 90 and 69 % yield, respectively, and were characterized by elemental analysis, ESI-MS, IR, ^1H and ^{13}C NMR spectroscopies and single crystal structure X-ray diffraction (for L^2). The infrared spectra (KBr disc) show strong bands at 2239 (L^1) cm^{-1} or 2249 (L^2) cm^{-1} which are assigned to $\nu(\text{C}\equiv\text{N})$, features that are in accordance with the formation of the cyanoethylated macrocycles. Other absorption bands corresponding to $\nu(\text{C}=\text{C})$ vibrations from the aryl groups occur, as expected, at *ca.* 1609, 1510 and 1456 cm^{-1} .

The ^1H NMR spectra of L^1 and L^2 confirm the integrity of the ligands and their stability in solution, also showing the chemical equivalence of the different segments of their structures, as one would expect for this kind of systems. In fact, the singlets at δ 4.37 (L^1) or 4.15 (L^2) are assigned to the $\text{O}-\text{CH}_2$ methylene protons while those at δ 3.69 (L^1) or 3.47 (L^2) are due to $\text{Ar}-\text{CH}_2-\text{N}$. The set of signals in the δ 2.17 – 2.84 (for L^1) or 2.35 – 2.77 (for L^2) range is attributable to the ethylenic fragments of the pendants. The aryl protons exhibit the expected patterns and the chemical shifts are also consistent with the proposed structures. In the ^{13}C spectra, the cyano carbon appears at δ 119.40 for L^1 and 119.34 for L^2 .

The coordination abilities of L^1 and L^2 towards Ag(I) were studied. The reactions of L^1 with silver nitrate in the 1:1 and 2:1 metal-to-ligand ratios, led to the formation of the mononuclear and the polymeric macrocyclic metal complexes $[AgL^1](NO_3)$ (**1**) and $[Ag_2(NO_3)_2L^1]_n$ (**2**), respectively (Scheme 2). The reaction of L^2 with silver nitrate in a 2:1 metal-to-ligand ratio (corresponding to a 1:1 molar ratio for the N_3 motif in this ligand and $AgNO_3$) led to the formation of the macrocyclic polymeric compound $\{[Ag_2L^2](NO_3)_2\}_n$ (**3**) (Scheme 2).

Compounds **1** - **3** were characterized by elemental analysis, IR, NMR spectroscopies, ESI-MS and single crystal X-ray diffraction. The cyano groups are clearly detected by their IR $\delta(C\equiv N)$ bands at *ca.* 2247 cm^{-1} . In their 1H NMR spectra, the singlets at δ 4.52 (**1**), 4.53 (**2**) or 4.16 (**3**) are assigned to the O- CH_2 methylene protons while those at δ 3.78 (**1**), 3.79 (**2**) or 3.46 (**3**) are due to Ar- CH_2 -N. The set of signals in the δ 2.55 – 2.93 (for **1**), 2.39 – 2.72 (for **2**) or 2.73 – 2.76 (for **3**) range is attributable to the ethylenic fragments of the pendants and the aryl groups are located in the range of 7.04 – 7.41 for **1**, 7.04 – 7.42 for **2** or 6.89 – 7.26 for **3**. Their ESI-MS spectra exhibit the silver-containing fragments $[AgL^1]^+$ (**1** and **2**) or $[Ag_2L^2(NO_3)]^+$ (**3**). Moreover, for **2** and **3**, metallic fragments resulting from the coordination of the solvent (DMSO) are also detected.

Compound L^2 (Fig 1) crystallized in the monoclinic space group $P2_1/c$, its asymmetric unit contains only half of the molecule and an inversion centre is located in the middle of the macrocycle. Bond lengths and angles are within the normal ranges. The distances between symmetrically equivalent amine N atoms are of 14.511(4), 17.722(5) and 18.302(5) Å, while those between the oxygen atoms are of 4.182(2) and 7.553(3) Å. The distance of 17.723(5) Å between the two bridge-head amine atoms (N1 and N1A) is shorter than that of the Schiff base compound L^{1a} (18.890(3) Å) [19b].

The asymmetric unit of compound $[AgL^1](NO_3)$ (**1**) comprises one unit of the cationic silver complex and one nitrate as counterion (Fig 2). The Ag cation is in a square-pyramidal coordination environment ($\tau_5 = 0.03$) [25] with the L^1 ligand

connecting the metal by means of the three *N*-amine atoms and the two oxygen atoms; the silver ion stands in the least-square basal plane formed by the O1, O2, N1 and N3 atoms. The average Ag–O bond length is of 2.572 Å, and that of Ag–N is of 2.474 Å. Intermolecular C–H $\cdots\pi$ interactions (average H \cdots centroid of 2.85 Å) could be found in the structure of **1** involving both aromatic rings.

Complex $[\text{Ag}_2(\text{NO}_3)_2\text{L}^1]_n$ (**2**) is a 2D coordination polymer (Fig 3) extended from a metal-organic coordination macrocycle made up of two silver cations, one L^1 ligand and two nitrate anions. The organic ligand acts as an octadentate $1\kappa^3\text{N}:2\kappa^2\text{O}, 2\kappa\text{N}, 3\kappa\text{N}, 4\kappa\text{N}$ chelator to four silver cations, two of them (Ag1 and Ag3) are included in the cavity of the ligands in a N_4O_2 octahedral location while the coordination geometries of the other two (Ag2 and Ag4) are better considered as N_2O_3 square-pyramids (τ_5 parameters of 0.22 and 0.09, respectively) with the oxygen atoms belonging to coordinated nitrate anions. Thus, one of the nitrate ligands binds the metal in a chelating fashion while the other one is monodentate.

The coordination polymer **2** (Fig 4) run along the crystallographic *a* and *b* axis generating infinite 2D layers made of Ag1 and Ag2 metal cations, or of Ag3 and Ag4. Moreover, the 2D framework structure of **2** can be viewed as a net composed of hexametallc 36-membered $\sim\text{Ag}_6(\text{N}_2\text{C}_3)_6\sim$ macrocyclic rings (A in Fig 4) in which the metal cations are linked by the *meta*-positioned cyanoethyl strands of four L^1 ligands, two of them furnishing one strand each and the remaining ones furnishing two strands. The distances involving the six silver ions in these rings range from 6.620(1) to 15.619(2) Å, the former being the minimum metal \cdots metal intralayer length found in this structure; the minimum interlayer one engages Ag1 and Ag4 and reaches 9.309(2) Å.

The asymmetric unit of $\{[\text{Ag}_2\text{L}^2](\text{NO}_3)_2\}_n$ (**3**) consists of one silver cation, half of a molecule of the L^2 ligand and a nitrate counter anion, an inversion centre being then located in the middle of the macrocycle (Fig 5). The organic group acts as an octadentate $1\kappa^3\text{N}, 2\kappa^3\text{N}, 3\kappa\text{N}, 4\kappa\text{N}$ chelator to the silver cations that rest in distorted square planar ($\tau_4 = 0.24$) [26] N_4 environments, each macrocycle bearing four

uncoordinated nitrile strands. The L^2 ligand can be viewed in the role of a bridge connecting to four metal cations which then extends along the crystallographic b and c axis leading to a zig-zag 2D network (Fig 6). The structure of **3** presents a more complex architecture as compared with that of **2**, derived from hexametallic 58-membered $\sim Ag_6(N_2C_3)_4(N_2C_{12}O_2)_2 \sim$ cyclic sets (B in Fig 6; the cyclic set is also represented in Figure S1) where the metal \cdots metal distances range from 7.9400(4) (the shortest Ag \cdots Ag distance found in **3**) to 25.722(1) Å.

The Ag-N bond distances in **3** range from 2.247(3) to 2.537(3) Å, the shorter one belonging to the metal- N_{nitrile} group. The C \equiv N bond distances of the coordinated and uncoordinated nitrile groups are quite similar [1.136(4) and 1.140(5) or 1.152(7) Å, respectively]. The distances between an amine N atom and its symmetrically equivalent analogue range from 15.676(4) to 16.748(3) Å and those between the oxygen atoms are of 4.487(3) and 5.800(3) Å, therefore indicating a clear shrinking of the cavity of L^2 upon coordination. The two silver ions in the cavity are 14.9270(6) Å apart, which is longer than the distance found in the silver N_8O_6 cryptand compound (14.666(1) Å) [27].

The TG and DTA curves for complexes **1-3** are shown in Fig. S2 (see Supplementary Information). The decomposition processes include three major weight losses, the final product being Ag_2O . In the curve of **1**, the first decomposition step (in the range 161 – 348 °C, 38.9 % loss) includes the decomposition of one NO_3^- , three nitrile strands and one $-C_2H_4N$ group of L^1 . The second step (temperature range of 348 - 410 °C) is assigned to the loss (5.8 %) of another $-C_2H_4N$ group. The last step within the range of 432 – 595 °C (36.8 % loss) corresponds to the decomposition of the left-over L^1 . In the case of **2**, the first sharp loss in the range of 169-188 °C is assigned to the decomposition of the two nitrate ligands according to the percentage of loss (calc 14.8 % for the two NO_3^-). The second step of loss (temperature range of 225 - 337 °C) is assigned to the decomposition of the nitrile strands of L^1 (calc 19.3 % for the three $-C_3H_4N$ groups). The last step is the decomposition of the left-over part of L^1 (30.0 % for $C_{16}H_{16}N_2O$). Compound **3** exhibits a mechanism of thermal

decomposition similar to the one presented by **1**: the first two steps (40.9 % loss) include the decomposition of the two NO_3^- , six nitrile stands and two $-\text{C}_2\text{H}_4\text{N}$ groups of L^2 ; the last step (41.8 % loss) is assigned to the decomposition of the left-over L^2 ($\text{C}_{36}\text{H}_{40}\text{N}_4\text{O}_3$, calc. 43.0 %).

Electrochemical behaviour

The electrochemical behaviours of complexes **1-3**, as well as of ligands L^1 and L^2 , were investigated by cyclic voltammetry (CV) and controlled potential electrolysis (CPE), at a platinum working electrode at 25 °C in a 0.2 M [$n\text{Bu}_4\text{N}$][BF_4]/NCMe solution. Complexes **1-3** exhibit one single-electron (as measured by CPE) irreversible reduction wave at potential values (Table 2) in the 0.06 to 0.15 V vs. SCE range, assigned to the $\text{Ag(I)} \rightarrow \text{Ag(0)}$ reduction (wave I^{red}). Upon scan reversal, after the cathodic process, an irreversible (with desorption) anodic wave (II^{ox}) at 0.32 – 0.39 V vs. SCE (Table 2) is observed, corresponding to the oxidation of cathodically generated metallic silver. In **2**, no Ag-Ag interaction, through the nitrile bridges [28], was detected by CV, on account of the distance between the silver ions.

1-3 also show one irreversible anodic wave in the range 0.93 to 1.32 V vs. SCE (Table 2), which can involve the ligands L^1 and L^2 . A typical cyclic voltammogram is exemplified in Figure 7.

In fact, L^1 and L^2 are also redox active, exhibiting a first irreversible oxidation wave at 0.74 and 0.98 V vs. SCE, respectively, followed by a reversible one at 1.03 and 1.22 V vs. SCE, correspondingly (Table 2, Figure 8).

Conclusion

Cyanoethyl-functionalized 17- and 42-membered macrocyclic compounds were easily synthesized by [1+1] or [2+2] condensations of the respective dialdehydes with diethylenetriamine followed by hydrogenation with KBH_4 and functionalization by acrylonitrile. They emerge as convenient N,N,N,O,O-pentapodal and double N,N,N-tripodal ligands towards silver ion.

Stable Ag(I) complexes were obtained (usually in good yields), two of which (**2** and **3**) of a polymeric nature, by simple reactions of silver nitrate with such ligands. They show interesting structures, which are markedly dependent on the molar ratios between the silver salts and the ligands, and on the structures of the ligands themselves: **1** is a mononuclear complex; **2** has one silver ion in the cavity of the ligand which is coordinated to other three silver ions by the three functionalized cyanoethyl strands thus generating an infinite 2D layer structure; **3** displays two silver ions in the cavity of the ligand which binds other two silver atoms by two cyanoethyl strands and, simultaneously, each silver cation in the cavity accepts a cyanoethyl strand, therefore generating an intricate architecture and extending the structure in infinite 2D zig-zag layers. Their thermal and electrochemical properties were also studied, allowing to compare their thermal stability, as well as their redox behaviour. It was also found that **L**¹ and **L**² are redox active.

Complexes **2** and **3** represent rare examples of stable silver cyanoethyl functionalized coronand polymeric compounds and the work provides good candidates for further assembly of metal ions with the functionalized macrocyclic compounds and deserves to be extended to other substituted macrocyclic metal complexes on attempting to study metal and ligand substituent effects, and to establish structure-composition relationships.

Acknowledgements

The authors are grateful for the financial support from the Foundation for Science and Technology (FCT), Portugal, and its programs (POCI, FEDER funded, Grant No. SFRH/BPD/24691/2005 and Project PEst-OE/QUI/UI0100/2013), the Science Foundation of China (21261002) and the Opening Project of Guangxi Key Laboratory of Petrochemical Resource Processing and Process Intensification Technology (K008).

The authors acknowledge the Portuguese NMR Network (IST-UTL Centre) for access to the NMR facility, and the IST Node of the Portuguese Network of

mass-spectrometry (Dr. Conceição Oliveira) for the ESI-MS measurements.

References

1. K. P. Guerra, R. Delgado, M. G. B. Drew, V. Felix (2006) *Dalton Trans.*, 4124.
2. L. Tei, A. J. Blake, P. A. Cooke, C. Caltagirone, F. Demartin, V. Lippolis, F. Morale, C. Wilson, M. Schroder (2002) *J. Chem. Soc., Dalton Trans.*, 1662.
3. L. Valencia, R. Bastida, M. del C. Fernandez-Fernandez, A. Macias, M. Vicente (2005) *Inorg. Chim. Acta*, **358**, 2618.
4. L. J. Barbour, S. L. De Wall, R. Ferdani, F. R. Fronczek, G. W. Gokel (2001) *Inorg. Chim. Acta*, **317**, 121.
5. M. C. Fernandez-Fernandez, R. Bastida, A. Macias, P. Perez-Lourido, L. Valencia (2006) *Inorg. Chem.*, **45**, 2266.
6. D. Kong, Y. Xie (2002) *Inorg. Chim. Acta*, **338**, 142.
7. (a) A. G. Herve, G. Jacob, R. Gallo (2006) *Chem. Eur. J.*, **12**, 3339; (b) Hai-Bing Xu, Hsiu-Yi Chao (2007) *Inorg. Chem. Commun.*, **10**, 1129; (c) L. J. Barbour, S. L. De Wall, R. Ferdani, F. R. Fronczek, G. W. Gokel (2001) *Inorg. Chim. Acta*, **317**, 121.
8. (a) B.-C. Tzeng, W.-C. Lo, C.-M. Che, S.-M. Peng, (1996) *Chem. Commun.*, 181; (b) P. Planinic, D. Matkovic-Calogovic, H. Meider, (1997) *J. Chem. Soc., Dalton Trans.*, 3445.
9. X. Zhu, Z. Ma, W. Bi, Y. Wang, D. Yuan, R. Cao (2008) *Cryst. Eng. Comm.*, **10**, 19.
10. M. E. Padilla-Tosta, J. M. Lloris, R. Martonez-Manez, A. Benito, J. Soto, T. Pardo, M. A. Miranda, M. D. Marcos, (2000) *Eur. J. Inorg. Chem.*, 741.
11. M. C. Fernandez-Fernandez, R. Bastida, A. Macias, P. Perez-Lourido, L. Valencia (2007) *Polyhedron*, **26**, 5317.
12. M. V. Baker, D. H. Brown, B. W. Skelton, A. H. White, (2000) *J. Chem. Soc., Dalton Trans.*, 4607.
13. M. L. Cable, J. P. Kirby, K. Sorasaene, H. B. Gray, A. Ponce (2007) *J. Am. Chem. Soc.*, **129**, 1474.
14. (a) E. Kimura, T. Ikeda, M. Shionoya, M. Shiro (1995), *Angew. Chem., Int. Ed.*, **34**, 663; (b) S. C. Rawle, P. Moore, N. W. Alcock (1992) *Chem. Commun.*, 684.
15. (a) Z. Ma, Z. Chen, R. Cao (2005) *Eur. J. Inorg. Chem.*, 2978; (b) Z. Ma, G. Ran, (2011) *J. Coord. Chem.*, **64**, 1446.
16. T. Koullourou, L. S. Natrajan, H. Bhavsar, S. J. A. Pope, J. Feng, J. Narvainen, R. Shaw, E. Scales, R. Kauppinen, A. M. Kenwright, S. Faulkner (2008) *J. Am. Chem. Soc.*, **130**, 2178.
17. (a) T. Koullourou, L. S. Natrajan, H. Bhavsar, S. J. A. Pope, J. Feng, J. Narvainen, R. Shaw, E. Scales, R. Kauppinen, A. M. Kenwright, S. Faulkner (2008) *J. Am. Chem. Soc.*, **130**, 2178; (b) L. Tei, A. J. Blake, V. Lippolis, C. Wilson, M. Schroder (2003) *Dalton Trans.*, 304.
18. (a) M. Napoli, C. Saturnino, E. I. Cianciulli, M. Varcamonti, A. Zanfardino, G.

- Tommonaro, P. Longo, (2013) *J. Organometallic Chem.* **725**, 46; (b) Y. Zhao, K. Chen, J. Fan, T. Okamura, Y. Lu, L. Luo, W. Sun, (2014), *Dalton Trans.*, **43**, 2252; (c) J. W. Rigoli, C. D. Weatherly, J. M. Alderson, B.T. Vo, J. M. Schomaker, (2013) *J. Am. Chem. Soc.*, **135**, 17238; (d) L. Maestre, W. M. C. Sameera, M. M. Diaz-Requejo, F. Maseras, P. J. Perez, (2013) *J. Am. Chem. Soc.*, **135**, 1338.
19. (a) K. R. Adam, L. F. Lindoy, H. C. Lip, John H. Rea, (1981), *J. Chem. Soc. Dalton Trans.*, 74; (b) Z. Ma, S.-X. Liu, (2003) *Chinese J. Struct. Chem.*, **22**, 553.
20. (a) A.J.L. Pombeiro, M.F.C. Guedes da Silva, M.A.N.D.A. Lemos, (2001) *Coord. Chem. Rev.*, **219**, 53; (b) M.E.N.P.R.A. Silva, A.J.L. Pombeiro, J.J.R. Fraústo da Silva, R. Herrmann, N. Deus, T.J. Castilho, M.F.C. Guedes da Silva, (1991) *J. Organometal. Chem.*, **421**, 75; (c) M.E.N.P.R.A. Silva, A.J.L. Pombeiro, J.J.R. Fraústo da Silva, R. Herrmann, M. Deus, R.E. Bozak, (1994) *J. Organometal. Chem.*, **480**, 81.
21. Bruker, *APEX2 & SAINT*. Madison, Wisconsin, USA, 2004.
22. G. M., Sheldrick, (1990) *Acta Cryst. Sec. A*, **46**, 467.
23. G. M., Sheldrick, (2008) *Acta Cryst. Sec. A*, **A64**, 112.
24. L. J., Farrugia, (1999) *J. Appl. Cryst.*, **32**, 837.
25. A.W. Addison, T.N. Rao, J. Reedijk, J. Van Rijn, G.C. Verschoor, (1984) *J. Chem. Soc. Dalton Trans.*, 1349.
26. L. Yang, D. R. Powell, R.P. Houser, (2007) *Dalton Trans.*, 955.
27. Z. Ma, R. Cao, (2005) *J. Mol. Struct.*, **738**, 137.
28. A.I.F. Venâncio, M.L. Kuznetsov, M.F.C. Guedes da Silva, L.M.D.R.S. Martins, J.J.R. Fraústo da Silva, A.J.L. Pombeiro, (2002) *Inorg. Chem.*, **41**, 6456.

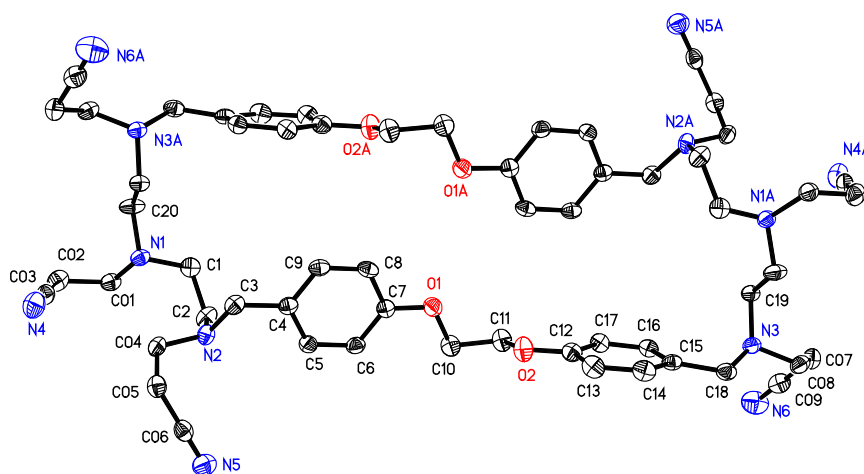


Fig. 1 ORTEP view of L^2 . Ellipsoids were drawn at 30 % probability. Symmetry operation to generate equivalent atoms: A) $-x, 1-y, 2-z$.

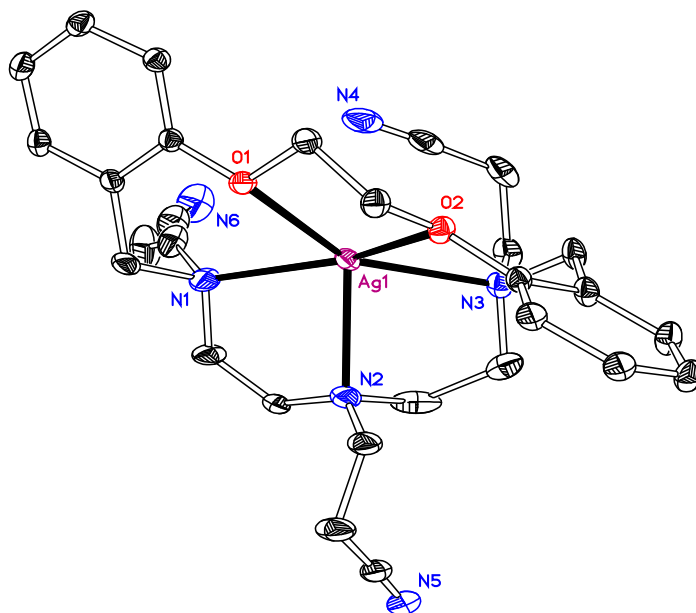


Fig. 2 Ortep diagram of $[Ag(L^1)]^+$ (**1**) with partial atom numbering scheme. Ellipsoids are drawn at 30 % probability. H atoms were omitted for clarity and only one of the disordered components is shown.

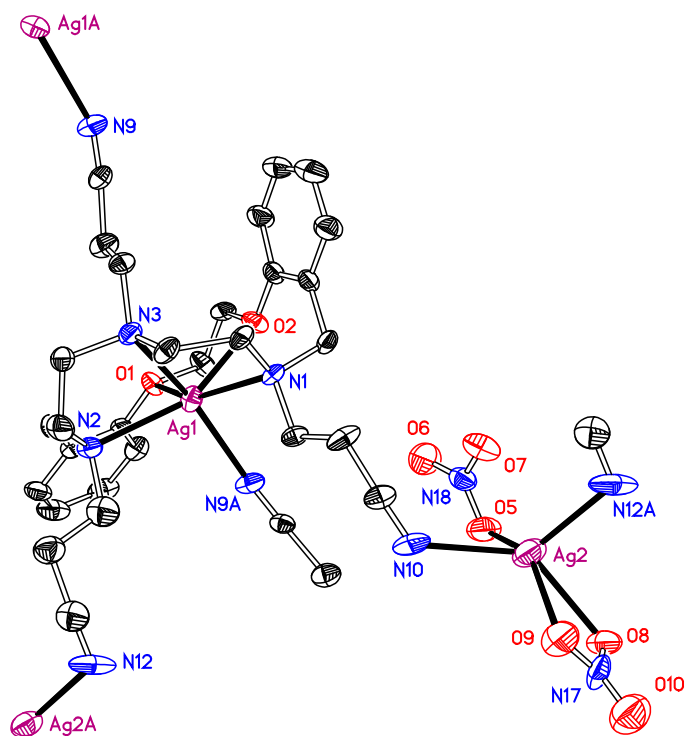


Fig. 3 Ortep diagram of $[Ag_2(NO_3)_2(L^1)]_n$ (**2**) with partial atom numbering scheme. Ellipsoids are drawn at 30 % probability. Symmetry operation to generate equivalent atoms: A) $1/2+x, 1-y, z$; B) $x, 1+y, z$; C) $x-1/2, 1-y, z$. H atoms were omitted for clarity and only one of the disordered components is shown.

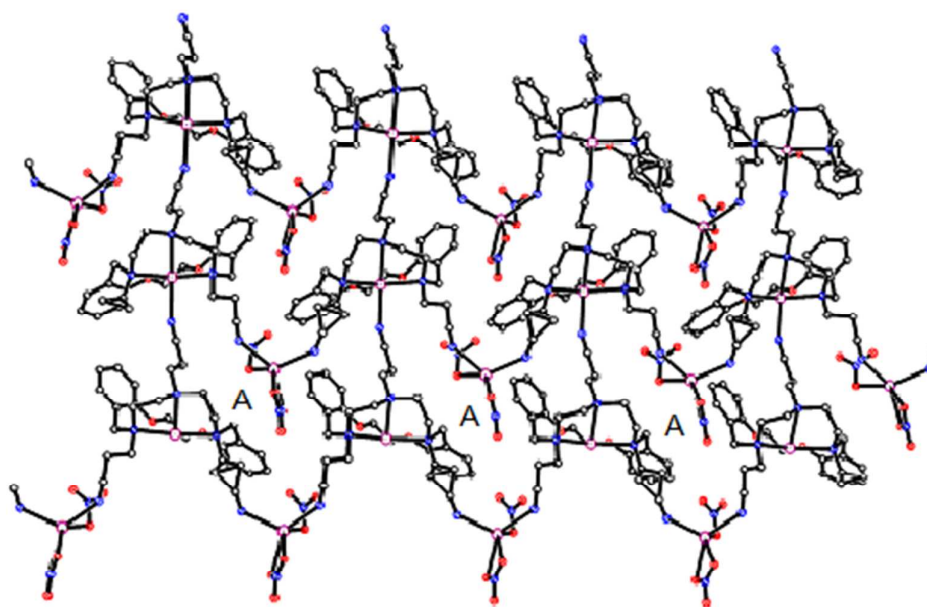


Fig. 4 Packing diagram of **2** viewed down the crystallographic *a* axis (H atoms were omitted for clarity).

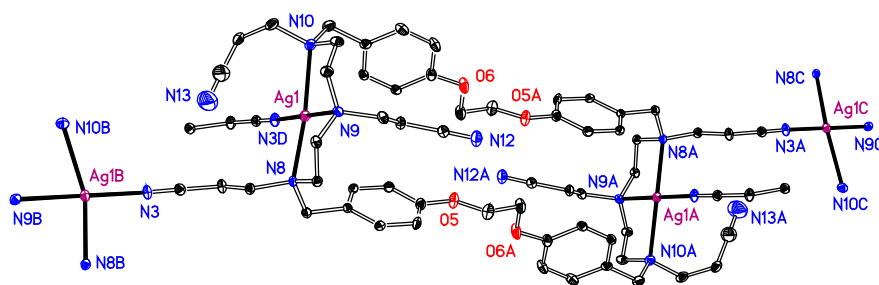


Fig. 5 ORTEP view of complex $\{[Ag_2(L^2)]^{2+}\}_n$ (**3**). Ellipsoids are drawn at 30 % probability. Symmetry operation to generate equivalent atoms: A) $2-x, -y, 1-z$; B) $x, 1/2-y, z-1/2$; C) $2-x, y-1/2, 3/2-z$. H atoms were omitted for clarity and only one of the disordered components is shown.

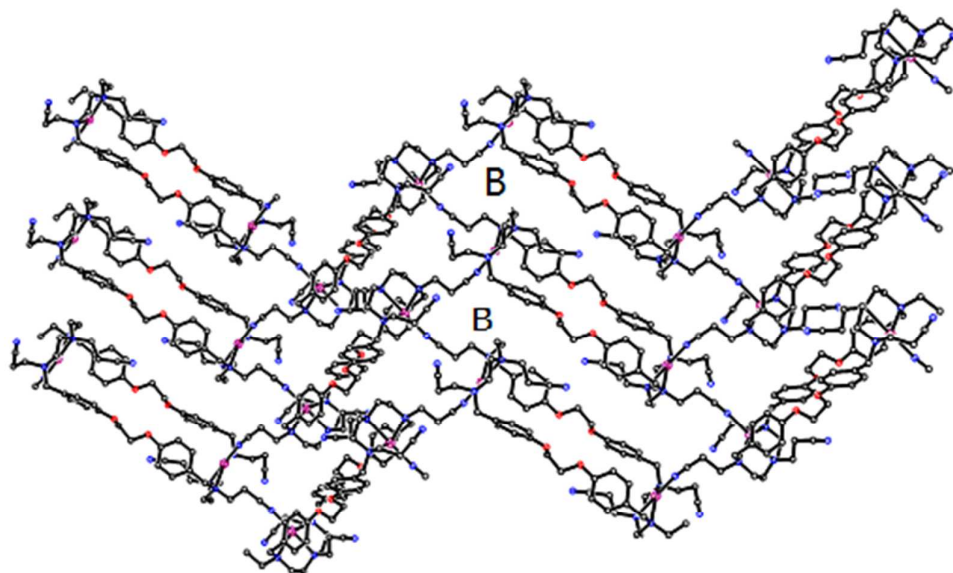


Fig. 6 Crystal packing diagram of **3** viewed down the crystallographic *a* axis (H atoms are omitted for clarity) showing the 2D metal-organic skeletons with trapped nitrate ions.

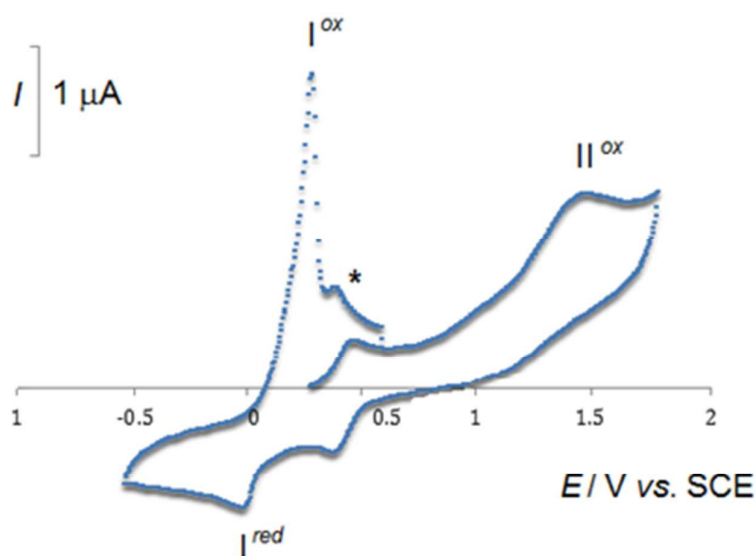


Fig. 7 Cyclic voltammogram of **1** in a 0.2 M [*t*Bu₄N][BF₄]/NCMe solution, at a Pt disc working electrode (*d* = 0.5 mm), run at a scan rate of 200 mVs⁻¹.

* [Fe(η^5 -C₃H₅)₂]^{0/+}

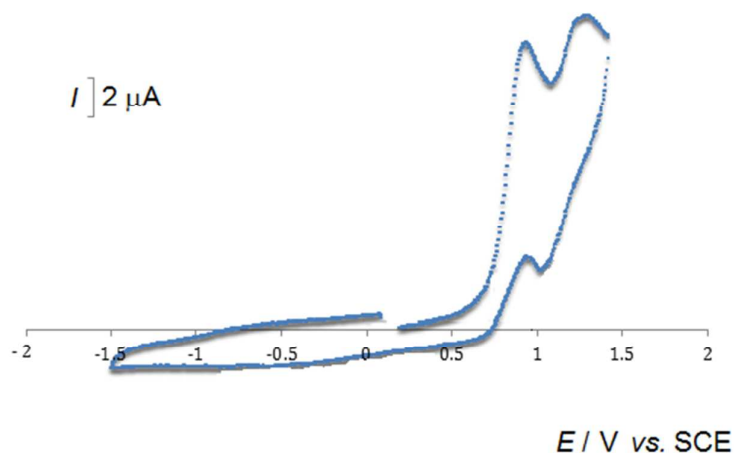


Fig. 8 Cyclic voltammogram of L^2 in a 0.2 M [n Bu $_4$ N][BF $_4$]/NCMe solution, at a Pt disc working electrode ($d = 0.5$ mm), run at a scan rate of 200 mVs $^{-1}$.

Table 1 Crystallographic data for compounds L^2 , **1**, **2** and **3**.

	L^2	1	2	3
Formula	C $_58$ H $_{72}$ N $_{12}$ O $_4$	C $_{29}$ H $_{36}$ AgN $_7$ O $_5$	C $_{29}$ H $_{36}$ Ag $_2$ N $_8$ O $_8$	C $_{29}$ H $_{36}$ AgN $_7$ O $_5$
Formula Weight	999.26	670.52	840.40	670.52
Crystal system	Monoclinic	Monoclinic	Orthorhombic	Monoclinic
Crystal size(mm)	0.40 × 0.30 × 0.10	0.37 × 0.32 × 0.26	0.31 × 0.20 × 0.14	0.41 × 0.19 × 0.15
Space group	$P2_1/c$	$P2_1/c$	$Pca2_1$	$P2_1/c$
a (Å)	16.377(4)	10.8117(6)	17.614(3)	10.3340(6)
b (Å)	17.142(5)	21.4389(13)	11.581(2)	34.337(2)
c (Å)	9.573(3)	14.0630(6)	31.048(6)	9.4266(3)
β (°)	93.614(8)	118.699(3)	90	106.526(3)
V (Å 3)	2682.3(13)	2859.2(3)	6333(2)	3206.7(3)
Z	2	4	8	4
D_{calc} (Mg m $^{-3}$)	1.237	1.557	1.762	1.389
μ (mm $^{-1}$)	0.080	0.758	1.300	0.676
$F(000)$	1068	1384	3391	1384

No. Rfl. unique	5128	8758	15211	5871
No. Rfl. observed	3850	7525	11699	5141
<i>R</i>	0.0533	0.0390	0.0506	0.0408
<i>wR</i>	0.1737	0.0926	0.1260	0.0915
<i>R for all</i>	0.0769	0.0473	0.0708	0.0473
<i>wR for all</i>	0.2010	0.0997	0.1390	0.0941
GOF	1.026	1.032	1.042	1.062
CCDC number	780499	936855	842196	780498

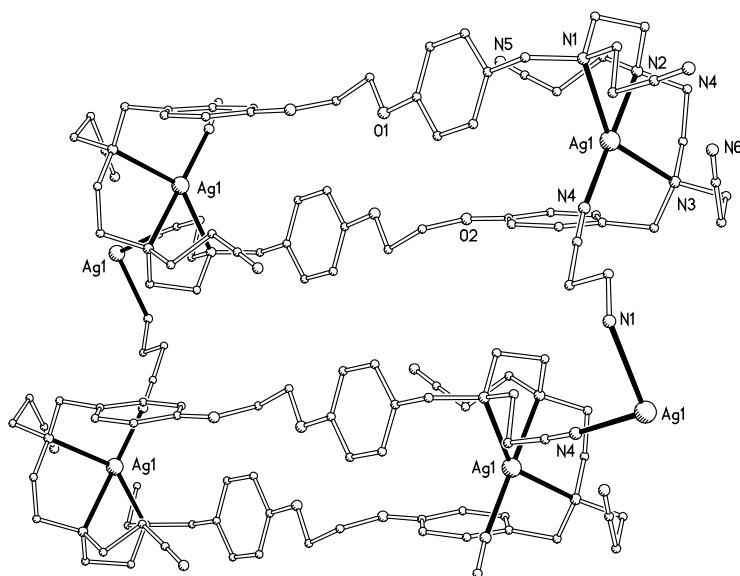
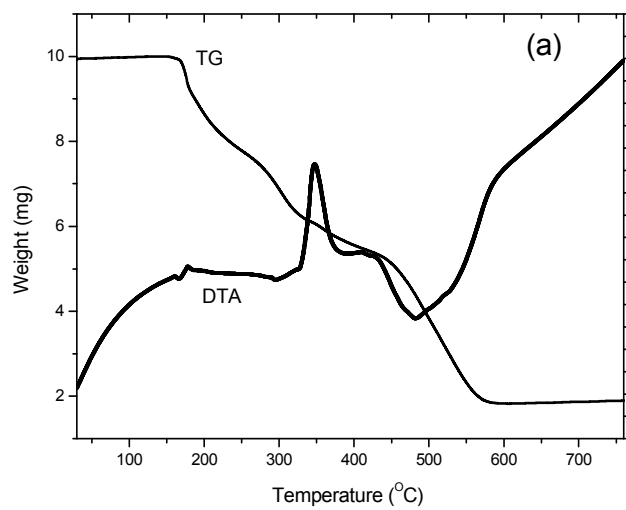
Table 2. Cyclic voltammetric data^a for compounds **L**¹, **L**², **1**, **2** and **3**.

Compound	E_p (I ^{red})	E_p (I ^{ox})	$E_{1/2}$ (II ^{ox})
L ¹	-	0.74	1.03
L ²	-	0.98	1.22
1 ^b	0.06	1.32	-
2 ^b	0.15	1.13	-
3 ^b	0.13	0.93	-

^a Potential values in Volt \pm 0.02 vs. SCE, in a 0.2 M [Bu₄N][BF₄]/NCMe solution, at a Pt disc working electrode determined by using the [Fe(η^5 -C₅H₅)₂]^{0/+} redox couple ($E_{1/2}^{ox}$ = 0.42 V vs. SCE [20]) as internal standard at a scan rate of 200 mVs⁻¹.

^b An anodic wave generated upon scan reversal following the reduction wave is observed at 0.32 (**1**), 0.34 (**2**) or 0.39 (**3**).

Supplementary Information

Fig. S-1 The cyclic hexametallate set of **3**

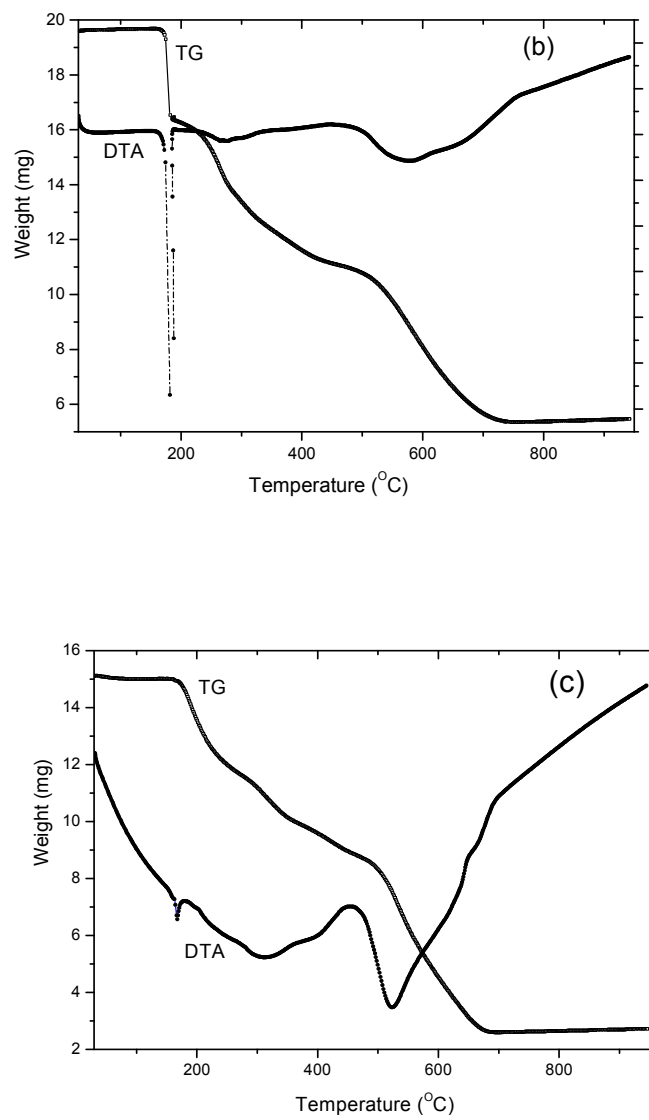
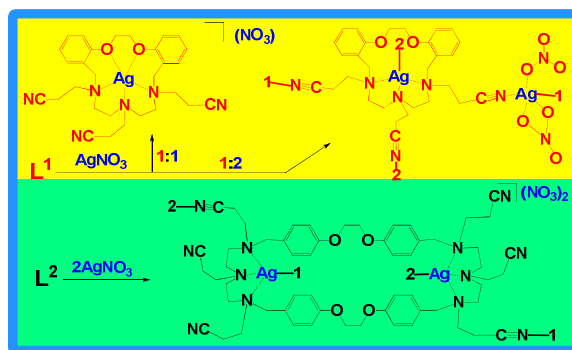


Fig. S-2 TG-DTA plots of **1** (a), **2** (b) and **3** (c)

Graphical abstract

Silver Coordination Polymers with Tri- and Hexacyanoethyl-functionalized Macrocyclic Ligands

Zhen Ma, Huaduan Shi, Xiuqiang Deng, M. Fátima C. Guedes da Silva, Luísa M. D. R. S. Martins, and Armando J. L. Pombeiro



Three silver(I) complexes, $[Ag(L^1)](NO_3)$ (**1**), $[Ag_2(NO_3)_2(L^1)]_n$ (**2**) and $\{[Ag_2(L^2)](NO_3)_2\}_n$ (**3**), were obtained by reaction of silver nitrate with the corresponding cyano-functionalized macrocyclic ligands. Their structures, thermal and electrochemical properties were studied.